Published OnlineFirst November 18, 2011; DOI: 10.1158/0008-5472.CAN-11-1891

Priority Report

Cancer Research

Stress-Regulated Transcription Factor ATF4 Promotes Neoplastic Transformation by Suppressing Expression of the INK4a/ARF Cell Senescence Factors

Michiko Horiguchi[1], Satoru Koyanagi[1], Akinori Okamoto[1], Satoshi O. Suzuki[2], Naoya Matsunaga[1], and Shigehiro Ohdo[1]

Abstract

Many cancers overexpress ATF4, a stress-induced transcription factor that promotes cell survival under hypoxic conditions and other stresses of the tumor microenvironment, but the potential contributions of ATF4 to oncogenesis itself have been little explored. Here, we report that ATF4 promotes oncogene-induced neoplastic transformation by suppressing the expression of cellular senescence-associated genes. Strikingly, primary embryo fibroblasts from *ATF4*-deficient mice were resistant to transformation by coexpression of H-ras^{V12} and SV40 large T antigen. In wild-type cells these oncogenes induced expression of the murine *Atf4* gene along with the cyclin-dependent kinase inhibitor *Cdkn2a*, which encodes the cell senescence-associated proteins p16INK4 and p19ARF. Elevated levels of ATF4 were sufficient to suppress expression of these proteins and drive oncogenic transformation. Conversely, genetic ablation of ATF4 led to constitutive expression of p16INK4a and p19ARF, triggering cellular senescence. Our findings define a central function for ATF4 in promoting oncogenic transformation by suppressing a central pathway of cellular senescence. *Cancer Res; 72(2); 395–401. ©2011 AACR.*

Introduction

cAMP-responsive element-binding proteins (CREB) and activating transcription factors (ATF) are basic region leucine zipper proteins, which act as transcriptional activators or repressors. Activating transcription factor-4 (ATF4), a member of the CREB/ATF family, is ubiquitously expressed throughout the body and is induced in response to various stress signals, including anoxia, hypoxia, endoplasmic reticulum stress, amino acid deprivation, and oxidative stress (1). The stress-induced expression of ATF4 causes adaptive responses in cells through regulating the expression of target genes involved in amino acid synthesis, differentiation, metastasis, angiogenesis, and drug resistance (1). Excessive expression of ATF4 is often observed in malignant tumors in humans and rodents (2). The highly expressed ATF4 is thought to facilitate tumor progression, because transcription of genes involved in tumor cell proliferation is modulated by ATF4 (3). However, the role of ATF4 in the malignant transformation of normal cells remains to be elucidated.

In this study, we found that embryonic fibroblasts prepared from *Atf4*-null (*Atf4*$^{-/-}$) mice showed resistance to oncogenic transformation induced by concomitant expression of protooncogenic RAS (H-ras^{V12}) and simian virus 40 large T antigen (SV40LT). On the basis of these findings, we further characterized the role of ATF4 during the malignant transformation. Our present results suggest that ATF4 acts as a suppressor of cellular senescence, thereby promoting oncogenic transformation.

Materials and Methods

Animals and cells

Heterozygous *Atf4*-null (*Atf4*+/−) mice and male balb/c Nu/Nu mice were cared for in accordance with the guidelines established by the Animal Care and Use Committee of Kyushu University (Fukuoka, Japan). Mouse embryonic fibroblasts (MEF) were prepared by standard techniques from littermate embryos of wild-type or *Atf4*$^{-/-}$ mice, and cells were maintained in DMEM (Sigma-Aldrich) supplemented with 10% FBS, 20 μmol/L β-mercaptoethanol, and 1× nonessential amino acid mix. For oncogenic transformation, MEFs were infected with 1×10^6 colony-forming units (cfu)/mL retroviral vectors expressing H-ras^{V12} and SV40LT (4). Anchorage-independent growth of oncogene-infected cells was evaluated by soft-agar colony formation assay. Nu/Nu mice were inoculated with cells (2.5×10^6 cells/mouse) infected with oncogenes. Tumor size was measured as described previously (5).

Authors' Affiliations: Department of [1]Pharmaceutical Sciences, Graduate School of Pharmaceutical Sciences, and [2]Department of Neuropathology, Graduate School of Medical Sciences, Kyushu University, Fukuoka, Japan

Note: Supplementary data for this article are available at Cancer Research Online (http://cancerres.aacrjournals.org/).

Corresponding Author: Shigehiro Ohdo, Department of Pharmaceutical Sciences, Graduate School of Pharmaceutical Sciences, Kyushu University, Fukuoka 812-8582, Japan. Phone: 81-92-642-6610; Fax: 81-92-642-6614; E-mail: ohdo@phar.kyushu-u.ac.jp

doi: 10.1158/0008-5472.CAN-11-1891

Published OnlineFirst November 18, 2011; DOI: 10.1158/0008-5472.CAN-11-1891

Cell-cycle analysis

Single cell suspension was prepared from tumor masses. Cells were incubated with 0.05 mg/mL propidium iodide for specific DNA staining. The samples were analyzed on the EPICS Elite flow cytometer (Beckman Coulter, Inc.). The total number of cells analyzed from each sample was 10,000.

Microarray gene expression analysis

The quality of extracted RNA was analyzed using an Agilent 2100 Bioanalyzer (Agilent Technologies). The cRNA was amplified and labeled using a Low Input Quick Amp Labeling Kit. Labeled cRNA was hybridized to a 44-K Agilent 60-mer oligo-microarray (Whole Mouse Genome Microarray Kit Ver.2.0). To identify up- or downregulated genes, we calculated Z-scores and ratios (nonlog scaled fold-change) from the normalized signal intensities of each probe. We set criteria for upregulated genes: Z-score 3.0 or more and ratio 2-fold or more; and for downregulated genes: Z-score −3.0 or less and ratio 0.5 or less. All microarray data were submitted to the Gene Expression Omnibus at the National Center for Biotechnology Information (accession number GSE31405). The functional analysis of the differentially expressed genes was done by using the Kyoto Encyclopedia of Genes and Genomes (KEGG) database on DAVID system (6).

Quantitative RT-PCR analysis

The complementary DNA (cDNA) was synthesized by reverse transcription using the ReverTra Ace quantitative real-time PCR (qRT-PCR) kit (Toyobo; ref. 7). Diluted cDNA samples were analyzed by RT-PCR using THUNDERBIRD SYBR qPCR Mix (Toyobo) and the 7500 RT-PCR system (Applied Biosystems). Sequences for PCR primers are described in Supplementary Table S1.

Luciferase reporter assay

The surround regions of CCAAT enhancer-binding protein (C/EBP)–ATF response element (CARE) in the mouse *p16Ink4a* and *p19ARF* promoter were amplified using DNA extracted from wild-type MEFs. The PCR products were ligated into a pGL4 Basic vector (*p16Ink4a*-Luc and p*19ARF*-Luc) as shown in Supplementary Fig. S1. The sequences of the CARE in luciferase vectors were mutated using a QuickChange site-directed mutagenesis kit (Strategene). Expression vectors for mouse ATF4 and C/EBPα were constructed as described previously (5). MEFs were transfected with 100 ng per well of reporter vectors and 500 ng per well of expression vectors using Lipofectamine LTX reagent (Invitrogen). phRL-TK vector (Promega) at 0.5 ng per well was also cotransfected as an internal control reporter.

Chromatin immunoprecipitation assays

MEFs were treated with 8% paraformaldehyde to cross-link the chromatin. Those samples were incubated with antibodies against ATF4, C/EBPα, and rabbit-IgG (Santa Cruz Biotechnology). Chromatin/antibody complexes were extracted using a protein G agarose kit (Roche). Isolated DNA was subjected to PCR using the following primer pair: 5′-GATTTCATACT-GGGCGTGGT-3′ and 5′-GCTGGGCTCCTTCTGGAC-3′.

Western blotting

Nuclear or cytoplasmic proteins prepared from tumor masses or MEFs were separated on SDS-polyacrylamide gels and transferred to polyvinylidene difluoride membranes. The membranes were reacted with antibodies against ATF4, p16INK4a, p19ARF, Retinoblastoma protein (Rb), p53, β-actin (Santa Cruz Biotechnology), or phosphorylated-Rb (Invitrogen). The immunocomplexes were reacted with horseradish peroxidase-conjugated secondary antibodies.

Histochemical analysis

Frozen tumor mass sections were prepared on day 14 after inoculation of mice with cells infected with oncogenes. Senescence-associated β-galactosidase (SA β-gal) positive cells were detected using a senescence detection Kit (BioVision). Terminal deoxynucleotidyl transferase-mediated dUTP nick end labeling (TUNEL) staining was carried out using the *in situ* Apoptosis Detection Kit (Takara). The percentage of SA β-gal–positive and TUNEL-positive cells was determined by counting the numbers of positive cells among at least 10,000 cells from each sample.

Statistical analysis

The statistical significance of differences among groups was analyzed by ANOVA and post-hoc Bonferroni comparisons. A 5% probability was considered significant.

Results and Discussion

To characterize the role of ATF4 in oncogenic transformation, we prepared MEFs from wild-type and $Atf4^{-/-}$ mice, and infected the cells concomitantly with retrovirus vectors expressing the H-ras^{V12} and the SV40LT (4). These oncogenes were equally expressed in wild-type and $Atf4^{-/-}$ cells (Supplementary Fig. S2A). Concomitant introduction of H-ras^{V12} and SV40LT significantly enhanced the growth of both wild-type and $Atf4^{-/-}$ cells, but the growth rate of $Atf4^{-/-}$ cells was modest as compared with that of wild-type cells (Supplementary Fig. S2B). Introduction of oncogenes also failed to induce anchorage-independent growth of $Atf4^{-/-}$ cells as shown by the formation of colonies on soft agar plate ($P < 0.01$, Fig. 1A), suggesting that the loss of ATF4 resulted in the phenotype resisting oncogene-induced malignant transformation. This notion was also supported by the fact that ectopic expression of ATF4 significantly enhanced oncogene-induced anchorage-independent growth of $Atf4^{-/-}$ cells ($P < 0.05$, Fig. 1B). Furthermore, overexpression of ATF4 in wild-type cells also accelerated oncogene-induced formation of colonies on soft agar plate ($P < 0.05$, Supplementary Fig. S2C). ATF4 seems to play as an essential role in oncogene-induced malignant transformation.

Next, we tested this hypothesis by using an implant model in mice. Equal numbers of wild-type or $Atf4^{-/-}$ cells infected with oncogene (H-ras^{V12} and SV40LT) were inoculated into the flanks of balb/c nu/nu mice. Although mice inoculated with wild-type cells infected with oncogenes showed a significant growth of tumor masses (Fig. 1C), mice inoculated with $Atf4^{-/-}$ cells showed no palpable tumor masses until 9 days after

Published OnlineFirst November 18, 2011; DOI: 10.1158/0008-5472.CAN-11-1891

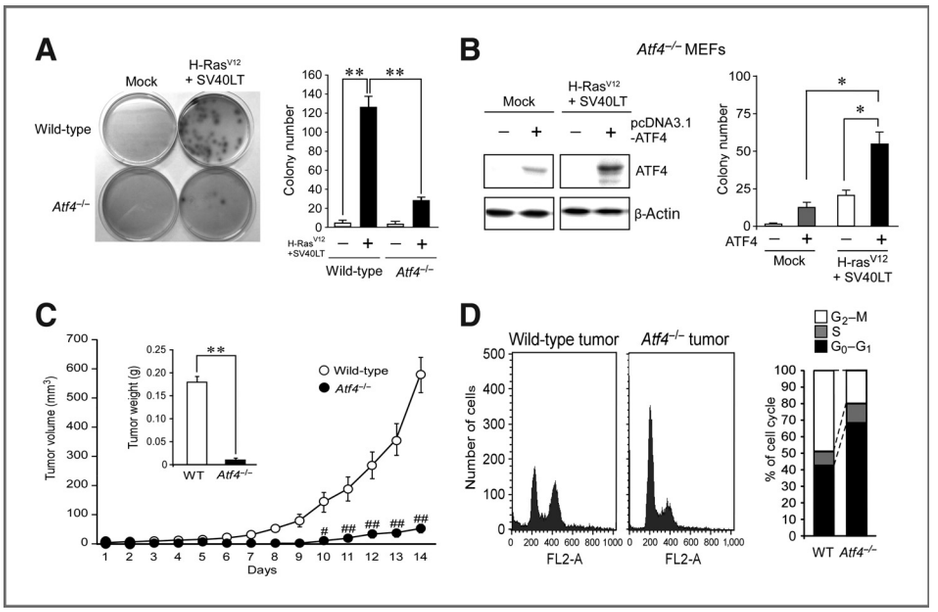

Figure 1. Resistance of *Atf4*$^{-/-}$ cells to oncogene-induced tumorigenesis. A, attenuated anchorage-independent growth of *Atf4*$^{-/-}$ cells with concomitant introduction of H-ras^{V12} and SV40LT (1×10^6 cfu/mL each). The cells infected with oncogenes were subjected to a soft agar colony formation assay. Colonies were stained with crystal violet. B, enhancement of oncogene-induced anchorage-independent growth of *Atf4*$^{-/-}$ cells by ectopic expression of ATF4. C, the growth of tumors in mice inoculated with wild-type (WT) or *Atf4*$^{-/-}$ cells infected with oncogenes. Inside, weight of tumor masses on day 14 after inoculation. D, the analysis of cell-cycle distribution of cells prepared from tumor masses formed by wild-type or *Atf4*$^{-/-}$ cells. All values are shown as means ± SE ($n = 3$–9). **, $P < 0.01$; *, $P < 0.05$ compared between the 2 groups. ##, $P < 0.01$; #, $P < 0.05$ compared with the wild-type group at the corresponding day.

inoculation. On day 14 after inoculation of cells, the average tumor weight in mice inoculated with the *Atf4*$^{-/-}$ cells was 9.28 ± 4.13 mg, representing a 94.82% reduction from that in mice inoculated with the wild-type cells (179.1 ± 11.97 mg; $P < 0.01$, Fig. 1C inside panel).

Comparison of flow cytometry (FACS) histograms from the wild-type and the *Atf4*$^{-/-}$ tumors also revealed a significant difference in the cell-cycle distribution between the genotypes. As compared with wild-type tumor cells, *Atf4*$^{-/-}$ cells were highly accumulated in the G_0–G_1 phase, whereas the population of the G_2–M phase of *Atf4*$^{-/-}$ cells was considerably smaller than that of wild-type cells (Fig. 1D). These results indicate that the loss of ATF4 attenuates the tumorigenicity of mouse fibroblasts and the G_0–G_1 phase arrest of the cell cycle underlies the resistance of *Atf4*$^{-/-}$ cells to oncogenic transformation.

To identify genes that enable *Atf4*$^{-/-}$ cells to resist oncogenic transformation, we carried out microarray analysis using RNA isolated from oncogene-introduced wild-type or *Atf4*$^{-/-}$ cells. A large number of genes would be induced or repressed by oncogenic stimuli. We thus focused on genes whose responsiveness to oncogenic stimuli was altered in *Atf4*$^{-/-}$ cells. On day 7 after concomitant introduction of H-ras^{V12} and SV40LT, 326 genes in *Atf4*$^{-/-}$ cells were differentially expressed as compared with wild-type cells. Among these genes, 216 genes in *Atf4*$^{-/-}$ cells were upregulated by oncogenic stimuli, whereas 110 genes were downregulated in oncogene-infected *Atf4*$^{-/-}$ cells (Supplementary Table S2). The functional analysis of the genes, done using KEGG database (6), showed that 12 biological pathways were enriched in a statistically significant manner ($P < 0.05$; Supplementary Table S3). Among these pathways, we further focused on the cell-cycle pathway because *Atf4*$^{-/-}$ cells introduced with oncogenes resulted in G_0–G_1 phase arrest (Fig. 1D). In this pathway, only Cdkn2a, a canonical inducer of cellular senescence, was highly expressed in *Atf4*$^{-/-}$ cells, despite a decrease in the expression of other cell-cycle regulatory genes (Table 1). These molecular findings prompted us to explore the possibility that ATF4 suppresses the transcription of cellular senescence-associated genes.

Recent studies have shown that tumor suppressor gene *Cdkn2a* acts as a canonical inducer of cellular senescence (8, 9). Cdkn2a generates several different transcript variants using different first exons and alternate polyadenylation sites (Fig. 2A; refs. 10, 11). The *p16Ink4a* variants encode structurally related protein isoforms that inhibit CDK4 kinase (9). The CDK4 inhibitor prevents phosphorylation of Rb by disrupting the activity of CDK4-Cyclin D complex, thereby causing G_1-phase arrest. The remaining transcript includes an alternate first exon located 20 kb upstream from the remainder of the *p16Ink4a* gene; this transcript contains an alternate open reading frame (ARF) that specifies a protein that is structurally unrelated to that of p16INK4a protein (10, 11). p19ARF (also known as p14ARF in humans) stabilizes p53 by sequestering MDM2, a protein responsible for degrading p53 (12). In spite of the structural and functional differences, p16INK4a and p19ARF play an important role in the cell cycle's G_1–S progression: The induction of these proteins is critical for causing cellular senescence (8, 9). Introduction of H-ras^{V12} and SV40LT

Published OnlineFirst November 18, 2011; DOI: 10.1158/0008-5472.CAN-11-1891

Table 1. Differentially expressed cell-cycle regulatory genes between oncogene-introduced wild-type and *Atf4*$^{-/-}$ cells

Gene symbol	Gene name	Z-score	Ratio	Genbank accession number
Cdkn2a	Cyclin-dependent kinase inhibitor 2A	4.074	11.038	NM_009877
Ttk	Ttk protein kinase	−3.252	0.031	NM_009445
Plk1	Polo-like kinase 1	−4.854	0.046	NM_011121
Ccnb1	Cyclin B1	−3.227	0.052	NM_172301
Espl1	Extra spindle polo-like 1	−3.164	0.056	NM_001014976
Ccna2	Cyclin A2	−3.268	0.074	NM_009828
Bub1	Budding uninhibited by benzimidazoles 1 homolog	−3.188	0.079	NM_009772
Cdc20	Cell division cycle 20 homolog (*Saccharomyces cerevisiae*)	−3.679	0.097	NM_023223
Ccnb2	Cyclin B2	−3.528	0.106	NM_007630
Mcm5	Minichromosome maintenance-deficient 5	−3.267	0.126	NM_008566
Cdk1	Cyclin-dependent kinase 1	−2.547	0.132	NM_007659

into wild-type cells significantly and consistently increased the levels of *Atf4* mRNA and its protein throughout the experimental period (Fig. 2B and C). Introduction of the oncogene also induced the expression of p16INK4a and p19ARF, but the induction was transient; mRNA levels of cellular senescence-associated genes reached a peak level from 1 to 2 days after oncogene introduction and decreased to basal level within 4 days (Fig. 2B and C). In contrast, introduction of H-ras^{V12} and

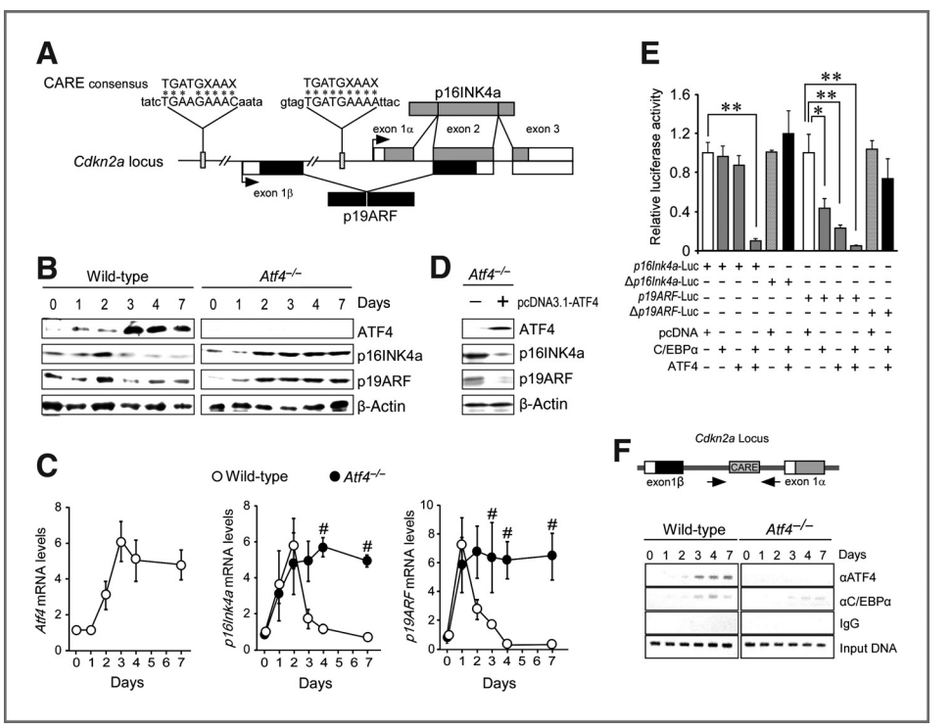

Figure 2. Transcriptional regulation of cellular senescence-associated genes by ATF4. A, location of CARE in the mouse *Cdkn2a* locus. The *Cdkn2a* gene has a unique first exon, exon 1α and 1β. The sequence inspection of *Cdkn2a* locus reveals 2 CAREs that match 8 bp and 9 bp, respectively, of the 9 bp consensus sequence TGATGXAAX (where X = A, T, or C). B and C, temporal profiles of protein (B) and mRNA (C) levels of ATF4, p16INK4a, and p19ARF in wild-type or *Atf4*$^{-/-}$ cells infected with oncogenes (H-ras^{V12} and SV40LT). D, suppressive action of ATF4 on oncogene-induced expression of p16INK4a and p19ARF in *Atf4*$^{-/-}$ cells. E, ATF4-C/EBPα-mediated repression of p16Ink4a and p19ARF transcription. Reporters contained either native (*p16Ink4a*-Luc and *p19ARF*-Luc) or mutated CARE (Δ*p16Ink4a*-Luc and Δ*p19ARF*-Luc). The presence or absence of reporter (100 ng) and expression plasmids (500 ng of ATF4 and C/EBPα) is indicated by (+) or (−). Activity of each reporter construct is relative to response in empty vectors (pcDNA3.1). F, temporal binding profiles of ATF4 and C/EBPα to the CARE in the *Cdkn2a* locus. Arrows indicate amplified area. All values are shown as means ± SE (n = 3–9). **, $P < 0.01$, compared between the 2 groups. #, $P < 0.05$ compared with wild-type group at the corresponding day.

Published OnlineFirst November 18, 2011; DOI: 10.1158/0008-5472.CAN-11-1891

SV40LT into *Atf4*$^{-/-}$ cells caused a significant and consistent increase in the expression of p16INK4a and p19ARF at both mRNA and protein levels ($P < 0.05$; Fig. 2B and C). The increase in the expression of p16INK4a and p19ARF in oncogene-introduced *Atf4*$^{-/-}$ cells was suppressed by ectopic expression of ATF4 (Fig. 2D), suggesting that excess ATF4 suppresses the expression of cellular senescence-associated genes induced by oncogenic stimuli.

ATF4 positively or negatively regulates the transcription of its target genes by forming homo- or hetero-dimers with Jun, AP-1, and C/EBP (13, 14). The dimerization partners seem to determine the diverse actions of ATF4. The hetero-dimerization of ATF4 with C/EBPα represses transcription on CARE (15). A consensus sequence of CARE was found in the upstream region of the mouse *p16Ink4a* gene (Fig. 2A). The sequence inspection of the upstream region of mouse *p19ARF* gene also revealed a CARE that matches 8 bp of the 9-bp consensus sequence TGATGXAAX (where X = A, T, or C). The CARE sequences were located at similar positions on the human CDKN2A locus. To explore whether ATF4 acts as a transcriptional repressor of cellular senescence-associated genes, we constructed 2 luciferase reporter vectors containing the CARE derived from the upstream region of mouse *p16Ink4a* and *p19ARF*. Neither ATF4 nor C/EBPα had a considerable effect on the luciferase activity of *p16Ink4a*-Luc, but cotransfection of *p16Ink4a*-Luc with both ATF4 and C/EBPα resulted in a 90% reduction of the luciferase activity (Fig. 2E). A similar transrepression was also found when cells were cotransfected of *p19ARF*-Luc with both ATF4 and C/EBPα (Fig. 2E). The transrepression effects of ATF4-C/EBPα on the *p16Ink4a*-Luc and *p19ARF*-Luc were dependent on the CAREs, because mutation of the sequences attenuated the suppressive action of ATF4-C/EBPα to the basal level (Fig. 2E).

The results of the chromatin immunoprecipitation analysis also revealed that the amounts of ATF4 binding to the Cdkn2a locus CARE located on the upstream of p16Ink4a in wild-type cells consistently increased from day 3 after introduction of H-ras^{V12} and SV40LT (Fig. 2F). On the other hand, no obvious binding of ATF4 to the Cdkn2a locus CARE was observed in oncogene-introduced *Atf4*$^{-/-}$ cells. The correlation between the binding activity of ATF4 to CARE and its transcriptional regulation of the *p16Ink4a* and *p19ARF* suggests that ATF4 functions as a transcriptional repressor of p16INK4a/ARF during oncogenic transformation.

During oncogenic transformation, cancer cells acquire genetic mutations that override the normal cell-cycle mechanism, resulting in abnormal proliferation. Failure of cells to override the mechanism often causes reversible cell-cycle arrest, apoptotic cell death, or cellular senescence (16). In contrast to reversible cell-cycle arrest, cellular senescence is defined by irreversible loss of proliferative potential, acquisition of characteristic morphology, and expression of specific biomarkers, such as SA β-gal (8, 17). On day 14, after inoculation of mice with oncogene-introduced *Atf4*$^{-/-}$ cells, a significant increase in the protein levels of p16INK4a and p19ARF was observed in tumor masses formed by *Atf4*$^{-/-}$ cells ($P < 0.05$, respectively; Fig. 3A). Induction of p16INK4a and p19ARF ultimately causes cellular senescence by modulating the activity of Rb and p53 (10–12). In fact, phosphorylation of Rb was significantly suppressed in tumor masses formed by *Atf4*$^{-/-}$ cells ($P < 0.05$; Fig. 3B), whereas a significant

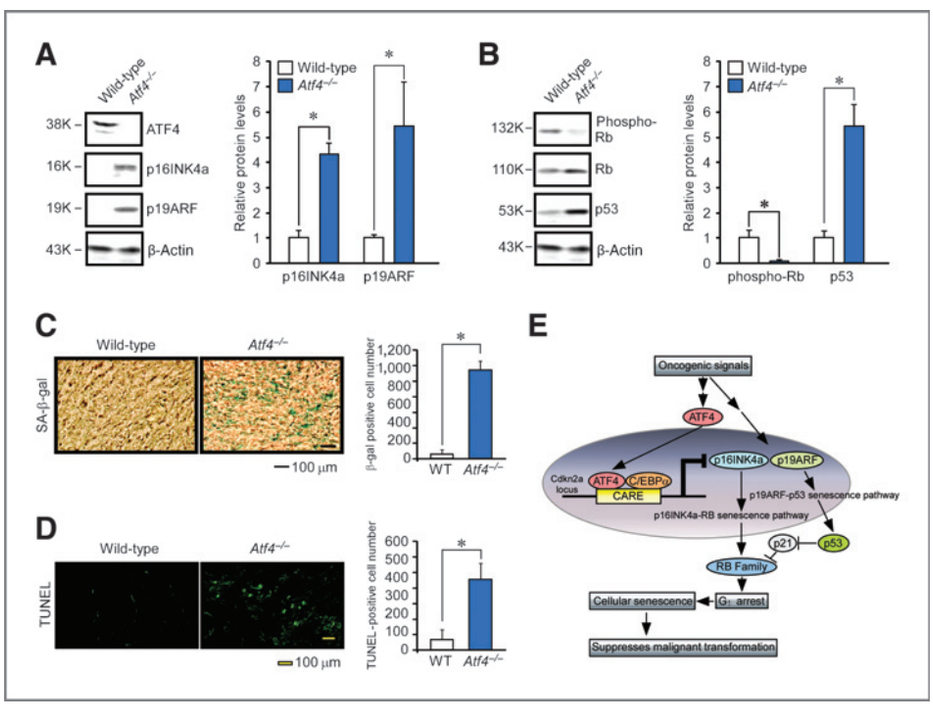

Figure 3. Induction of cellular senescence in tumor masses formed by *Atf4*$^{-/-}$ cells. A, the protein abundance of p16INK4a and p19ARF in tumor masses on day 14 after inoculation of mice with wild-type or *Atf4*$^{-/-}$ cells infected with oncogenes (H-ras^{V12} and SV40LT). B, the abundance of phosphorylated Rb (Phospho Rb) and p53 in tumor masses on day 14 after inoculation of mice with wild-type or *Atf4*$^{-/-}$ cells infected with oncogenes. **, $P < 0.01$; *, $P < 0.05$ compared between the 2 groups. C and D, the SA β-gal (C) and TUNEL (D) staining cells in tumor masses on day 14 after inoculation of mice with with wild-type or *Atf4*$^{-/-}$ cells infected with oncogenes. E, schematic mechanism of promotional action of ATF4 to oncogenic transformation by suppressing cellular senescence. All values are shown as means ± SE ($n = 3$–9). **, $P < 0.01$; *, $P < 0.05$, compared between the 2 groups.

Published OnlineFirst November 18, 2011; DOI: 10.1158/0008-5472.CAN-11-1891

accumulation of p53 was detected in *Atf4*$^{-/-}$ tumors ($P < 0.05$; Fig. 3B). Similar decrease in the levels of phosphorylated Rb and accumulation of p53 protein was also detected when cultured *Atf4*$^{-/-}$ cells were infected with H-ras^{V12} and SV40LT ($P < 0.05$, respectively; Supplementary Fig. S3). These results suggest that ATF4 acts to suppress cellular senescence during oncogenic transformation. This notion was also supported by the fact that the number of SA β-gal positive-cells in tumor masses formed by *Atf4*$^{-/-}$ cells was significantly higher than that in tumor masses formed by wild-type cells ($P < 0.05$; Fig. 3C). Furthermore, the number of TUNEL-positive cells, as an index of apoptotic cell death, also increased in tumor masses formed by *Atf4*$^{-/-}$ cells ($P < 0.05$; Fig. 3D). Because mice inoculated with *Atf4*$^{-/-}$ cells introduced with oncogenes showed a modest tumorigenicity (Fig. 1C), the induction of cellular senescence and apoptotic cell death seemed to be associated with modest tumor formation of *Atf4*$^{-/-}$ cells.

In this study, we used retrovirus vectors expressing SV40LT as a transforming agent, together with H-ras^{V12}. Because SV40LT inactivates p53 and prevents the phosphorylation of Rb by protein–protein interaction (18, 19), the SV40LT-transduced cells are thought to be insensitive to growth arrest by p16INK4a and p19ARF. Inactivation of the growth-suppressive properties of p53 has been shown to be essential for immortalization of MEFs by SV40LT (18). Concomitant introduction of H-ras^{V12} and SV40LT induced the expression of p53 in *Atf4*$^{-/-}$ cells, so that the amount of p53 proteins in oncogene-introduced *Atf4*$^{-/-}$ cells was much greater than that in wild-type cells (Supplementary Fig. S3). The largest amount of p53 protein in oncogene-introduced wild-type cells was precipitated together with SV40LT (Supplementary Fig. S4). However, a large amount of p53 protein in *Atf4*$^{-/-}$ cells was unable to be precipitated together with SV40LT, suggesting that extensive expression of p53 in oncogene-introduced *Atf4*$^{-/-}$ cells overrides the binding capacity of SV40LT, and allows induction of cellular senescence.

The present findings suggest the mechanism by which ATF4 promotes oncogenic transformation by suppressing the expression of cellular senescence-associated proteins (Fig. 3E). ATF4, p16INK4a, and p19ARF are expressed in response to oncogenic stimuli, but in turn, an overabundance of ATF4 suppresses the expression of these cellular senescence-associated proteins through binding to the CARE in the *Cdkn2a* locus. Decreases in the levels of cellular senescence-associated proteins restore stabilization of p53 by p19ARF and prevention of Rb hyperphosphorylation by p16INK4a, thus transforming cells so as to increase proliferation and oncogenic potentials. In fact, downregulation of *Cdkn2a* by siRNA enhanced oncogene-induced anchorage-independent growth of *Atf4*$^{-/-}$ cells (Supplementary Fig. S5). ATF4 is highly expressed in malignant tumors not only in rodents but also in humans (2). During oncogenic transformation of human cells, ATF4 may also play a role in overriding the normal cell-cycle mechanism, resulting in abnormal proliferation.

Disclosure of Potential Conflicts of Interest

No potential conflicts of interest were disclosed.

Acknowledgments

The cDNAs of H-ras^{V12} and SV40LT were kindly provided by Dr. Kitanaka (Yamagata University) and Dr. Sugano (Tokyo University), respectively. The authors thank the technical support from the Research Support Center, Graduate School of Medical Sciences, Kyushu University and Mr. Steven Sabotta for proofreading the paper.

Grant Support

This study was partially supported by a Grant-in-Aid for Scientific Research [(B) S. Ohdo, S. Koyanagi, N. Matsunaga, 21390047] from the Japan Society for the Promotion of Science.

Received June 6, 2011; revised October 13, 2011; accepted November 10, 2011; published OnlineFirst November 18, 2011.

References

1. Ameri K, Harris AL. Activating transcription factor 4. Int J Biochem Cell Biol 2008;40:14–21.
2. Ye J, Kumanova M, Hart LS, Sloane K, Zhang H, De Panis DN, et al. The GCN2-ATF4 pathway is critical for tumour cell survival and proliferation in response to nutrient deprivation. EMBO J 2010;29:2082–96.
3. Bi M, Naczki C, Koritzinsky M, Fels D, Blais J, Hu N, et al. ER stress-regulated translation increases tolerance to extreme hypoxia and promotes tumor growth. EMBO J. 2005;24:3470–81.
4. Kakumoto K, Sasai K, Sukezane T, Oneyama C, Ishimaru S, Shibutani K, et al. FRA1 is a determinant for the difference in RAS-induced transformation between human and rat fibroblasts. PNAS 2006;103:5490–5.
5. Okazaki F, Matsunaga N, Okazaki H, Utoguchi N, Suzuki R, Maruyama K, et al. Circadian rhythm of transferrin receptor 1 gene expression controlled by c-Myc in colon cancer-bearing mice. Cancer Res 2010;70:6238–46.
6. Horiguchi M, Kim J, Matsunaga N, Kaji H, Egawa T, Makino K, et al. Glucocorticoid-dependent expression of O(6)-methylguanine-DNA methyltransferase gene modulates dacarbazine-induced hepatotoxicity in mice. J Pharmacol Exp Ther 2010;333:782–7.
7. Kanehisa M, Goto S, Kawashima S, Nakaya A. The KEGG databases at GenomeNet. Nucleic Acids Res 2002;30:42–6.
8. Collado M, Serrano M. Senescence in tumours: evidence from mice and humans. Nat Rev Cancer 2010;10:51–7.
9. Kim WY, Sharpless NE. The regulation of INK4/ARF in cancer and aging. Cell 2006;127:265–75.
10. Kamijo T, Zindy F, Roussel MF, Quelle DE, Downing JR, Ashmun RA, et al. Tumor suppression at the mouse INK4a locus mediated by the alternative reading frame product p19ARF. Cell 1997;91:649–59.
11. Sharpless NE. INK4a/ARF: a multifunctional tumor suppressor locus. Mutat Res 2005;576:22–38.
12. Sherr CJ. Divorcing ARF and p53: an unsettled case. Nat Rev Cancer 2006;6:663–73.
13. Gachon F, Gaudray G, Thebault S, Basbous J, Koffi JA, Devaux C, et al. The cAMP response element binding protein-2 (CREB-2) can interact with the C/EBP-homologous protein (CHOP). FEBS Lett 2001;502:57–62.
14. Kato Y, Koike Y, Tomizawa K, Ogawa S, Hosaka K, Tanaka S, et al. Presence of activating transcription factor 4 (ATF4) in the porcine anterior pituitary. Mol Cell Endocrinol 1999;154:151–9.

Published OnlineFirst November 18, 2011; DOI: 10.1158/0008-5472.CAN-11-1891

15. Kilberg MS, Shan J, Su N. ATF4-dependent transcription mediates signaling of amino acid limitation. Trends Endocrinol Metab 2009;20:436–43.
16. Hanahan D, Weinberg RA. Hallmarks of cancer: the next generation. Cell 2011;144:646–74.
17. Collado M, Gil J, Efeyan A, Guerra C, Schuhmacher AJ, Barradas M, et al. Tumour biology: senescence in premalignant tumours. Nature 2005;436:642.
18. Zhu JY, Abate M, Rice PW, Cole CN. The ability of simian virus 40 large T antigen to immortalize primary mouse embryo fibroblasts cosegregates with its ability to bind to p53. J Virol 1991;65:6872–80.
19. Ewen ME, Ludlow JW, Marsilio E, DeCaprio JA, Millikan RC, et al. An N-terminal transformation-governing sequence of SV40 large T antigen contributes to the binding of both p110Rb and a second cellular protein, p120. Cell 1989;58:257–67.

Published OnlineFirst November 18, 2011; DOI: 10.1158/0008-5472.CAN-11-1891

Cancer Research
The Journal of Cancer Research (1916–1930) | The American Journal of Cancer (1931–1940)

AACR American Association for Cancer Research

Stress-Regulated Transcription Factor ATF4 Promotes Neoplastic Transformation by Suppressing Expression of the INK4a/ARF Cell Senescence Factors

Michiko Horiguchi, Satoru Koyanagi, Akinori Okamoto, et al.

Cancer Res 2012;72:395-401. Published OnlineFirst November 18, 2011.